THE JOURNAL OF PHYSICAL CHEMISTRY Letters

pubs.acs.org/JPCL Letter

Design Rules to Maximize Charge-Carrier Mobility along Conjugated Polymer Chains

Suryoday Prodhan,* Jing Qiu, Matteo Ricci, Otello M. Roscioni, Linjun Wang,* and David Beljonne*

Cite This: J. Phys. Chem. Lett. 2020, 11, 6519−6525 Read Online

ACCESS | Metrics & More | Article Recommendations | Supporting Information

ABSTRACT: The emergence of polymeric materials displaying high charge-carrier mobility values despite poor interchain structural order has spawned a renewal of interest in the identification of structure−property relationships pertaining to the transport of charges along conjugated polymer chains and the subsequent design of optimized architectures. Here, we present the results of intrachain charge transport simulations obtained by applying a robust surface hopping algorithm to a phenomenological Hamiltonian parametrized against first-principles simulations. Conformational effects are shown to provide a clear signature in the temperature-dependent charge-carrier mobility that complies with recent experimental observations. We further contrast against molecular crystals the evolution with electronic bandwidth and electron−phonon interactions of the room-temperature mobility in polymers, showing that intrachain charge-carrier mobility values in excess of 100 $cm^2/(V\ s)$ can be achieved through a proper chemical engineering of the backbones.

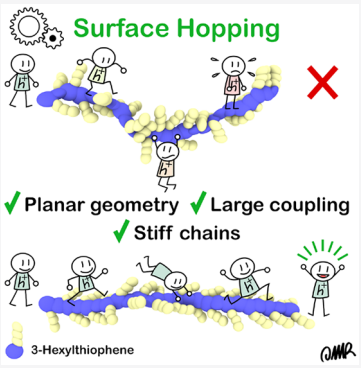

Charge transport is a key process in the working mechanism of a wide range of optoelectronic applications based on organic semiconductors.[1,2] In molecular materials, the motion of excess charge carriers is often modeled either in real space as successive hops between molecular units or in momentum space using a band model.[3,4] These are, however, limiting cases with static and/or dynamic energetic (local) and positional (nonlocal) disorders acting in synergy to spatially confine the charge, all the way from extended to localized states. The resulting crossover from band to hopping regime can be handled only by simultaneously solving the nuclear and electronic equations of motion, either in a full quantum mechanical way[5] or through a mixed quantum−classical scheme.[6−9]

The situation is, nevertheless, far more complex in conjugated polymers, namely because of the large anisotropy in charge transport, with large though-bond interactions along the conjugated backbone (mediating intrachain transport) versus weak through-space interactions between the backbones (driving interchain transport). Most of the present theoretical models rest on the assumption that high-mobility polymers consist of spatially close semicrystalline domains interconnected by "tie chains".[10,11] Overall, charge transport in these systems is a multiscale process where the macroscopic transport is limited by the amorphous domains and exhibits hopping-type transport behavior.[12] Consequently, earlier approaches for improving the charge transport properties in conjugated polymers primarily concentrated on enhancing the interchain interactions in highly crystalline materials,[13,14] very similar to the approach devised for molecular crystals.[15,16] For instance, the hole mobility of poly(2,5-bis(3-alkylthiophen-2-yl)thieno[3,2-*b*]thiophene) (PBTTT), $\mu \approx 1\ cm^2/(V\ s)$, gets enhanced by an order of magnitude compared to that of poly(3-hexylthiophene) (P3HT) and poly(5,5′- bis(3-alkyl-2-thienyl)-2,2′-bithiophene) (PQT) because of improved side-chain registry. Kline et al. have shown that μ can significantly increase with molecular weight in regioregular P3HT;[17] they have proposed that transport is restricted by the grain boundaries in low molecular weight polymers comprising rod-like nanocrystallites, while in high molecular weight polymers, long chains bridge the ordered domains.[18] Pulse radiolysis time-resolved microwave conductivity measurements on various polymers by Grozema et al. have suggested transport is unhindered over small length scales and the mobility can be comparable to that of inorganic semiconductors.[19] Cook and co-workers have recently reported charge mobility as high as 86 $cm^2/(V\ s)$ along a single polyfluorene chain employing a pulse radiolysis technique.[20] Over the past few years, experimental and theoretical studies have indicated that high μ values can be achieved in novel conjugated polymer architectures despite poor interchain registry.[21,22] These disordered or even seemingly amorphous, high-mobility, donor−acceptor type conjugated copolymers have emerged with charge mobility greater than 1 $cm^2/(V\ s)$,[23−25] thanks to their extended persistence lengths associated

Received: June 9, 2020
Accepted: July 21, 2020
Published: July 21, 2020

https://dx.doi.org/10.1021/acs.jpclett.0c01793
J. Phys. Chem. Lett. 2020, 11, 6519−6525

with the high polymer backbone rigidity, and extended conjugation via fused aromatic rings.[12] Recent optical spectroscopic studies of poly(indacenodithiophene-*alt*-benzothiadiazole) (IDTBT) type polymers, with $\mu \approx 2$ cm^2/(V s), have revealed that only few close contacts between chains allow for three-dimensional percolation network with charge transport being primarily intrachain in these copolymers.[26]

Charge transport in conjugated polymeric materials is a complex multiscale process, as realistic polymer chains involve multiple chromophores delineated by structural or chemical defects and because both intra- and interchain motion likely coexist. Here, motivated by the emergence of novel architectures with high intrachain charge-carrier mobility, we address the question of what is the microscopic limit to charge transport along conjugated polymer backbones. Although fundamental and timely, this question has surprisingly not been addressed in a comprehensive way yet. Previous charge transport simulations in polymers have either assumed incoherent hopping between conformational subunits[27,28] or focused on the electronic degrees of freedom while ignoring feedback effects from the nuclei, thus not incorporating polaronic effects.[29] Recently, Schmidt and co-workers have carried out first-principles calculations on P3HT employing the Kubo formalism and Holstein Hamiltonian, but considering a prefect crystalline structure.[30] Binder and co-workers have recently studied exciton dynamics mediated by torsional fluctuations in oligothiophene and oligo(para-phenylene vinylene) systems using multi-layer multi-configuration time-dependent Hartree (ML-MCTDH) method, revealing a temperature dependence similar to that reported in the present study. However, a direct comparison is not easy as motion of charges and excitons are governed by different interactions, being short-range for the former but long-range for the latter.[31−33] While a fully quantum-mechanical treatment of both nuclear and electronic degrees of freedom is computationally prohibitive, especially as one aims (as here) at exploring a large chemical and parameter space, charge transport can instead be modeled through a mixed quantum−classical dynamics approach, within model (Holstein−Peierls type)[6,34] or atomistic[35] Hamiltonians, which treats the nuclear motion classically and the electron dynamics quantum-mechanically. This is a reasonable approximation, because the temperature dependence of the mobility primarily stems from low-frequency vibrations with wavenumber below 100 cm^{-1}[36] (note that at ultralow temperature, quantum effects like tunneling may come into the picture,[37,38] and we have deliberately refrained from entering into this regime).

Here, we present a simplified but physically sound model that captures the important effects of both local and nonlocal electron−phonon interactions associated with conformational motion to explore the (temperature-dependent) charge-carrier mobility in single conjugated polymer chains across a broad parameter space. For this purpose, we resort to a crossing-corrected variant[39,40] of Tully's fewest switches surface hopping algorithm[41] that incorporates nonadiabatic transition between different adiabatic potential energy surfaces (PESs). This state-of-the-art technique can efficiently deal with complex surface crossings in extended systems[42] (methodology in detail is given in the Supporting Information). The dynamics of the system is described by an ensemble of independent trajectories, where each trajectory occupies an "active" PES at individual time steps. Along each trajectory, the electronic wave function $|\Phi(t)\rangle$ is propagated via the time-dependent Schrödinger equation (TDSE) $\partial|\Phi(t)\rangle/\partial t = H_e|\Phi(t)\rangle/\imath\hbar$. In the adiabatic basis representation $\{\phi_i(r;\mathbf{R}(t))\}$ ($|\Phi(t)\rangle = \sum_i c_i(t)|\phi_i(r;\mathbf{R}(t))\rangle$), this yields

$$\dot{c}_i(t) = c_i(t)E_i(\mathbf{R}(t))/\imath\hbar - \sum_j c_j(t)\dot{\mathbf{R}}(t)\cdot\mathbf{d}_{ij}(\mathbf{R}(t)) \tag{1}$$

$\mathbf{d}(\mathbf{R}(t))$ being the nonadiabatic coupling vector. $\mathbf{R}$ represents the corresponding coordinates of the nuclear degrees of freedom under study, and its dynamics on the active PES is modeled by the Langevin equation

$$M\ddot{\mathbf{R}} = -V' - \gamma M\dot{\mathbf{R}} + \xi \tag{2}$$

where $-V'$ is the effective force on the active PES, M the mass equivalent corresponding to the classical nuclear degrees of freedom, γ the friction coefficient, and ξ a Markovian Gaussian random force (for details, see ref 6). Stochastic hops between adiabatic PESs are implemented to achieve the internal consistency; that is, the fraction of trajectories on each PES should agree with the corresponding quantum population obtained by the TDSE.[41] Mean-squared displacement (MSD) is then calculated by

$$\mathrm{MSD}(t) = \frac{1}{N_{\mathrm{traj}}}\sum_i^{N_{\mathrm{traj}}} \langle\phi_a^{(i)}(t)|r^2|\phi_a^{(i)}(t)\rangle - \left[\frac{1}{N_{\mathrm{traj}}}\sum_i^{N_{\mathrm{traj}}} \langle\phi_a^{(i)}(t)|r|\phi_a^{(i)}(t)\rangle\right]^2 \tag{3}$$

where N_{traj} is the number of independent trajectories and $|\phi_a^{(i)}(t)\rangle$ is the active state at time t for the ith trajectory; in the current study, $N_{\mathrm{traj}} = 10\,000$ is chosen to obtain a smooth time evolution profile of MSD(t). Linear evolution of MSD(t) signifies that an equilibrium diffusion regime is attained, and the charge mobility can then be computed from the diffusion coefficient (D) using the Einstein relation

$$D = \frac{1}{2}\lim_{t\to\infty}[\mathrm{d}(\mathrm{MSD}(t))/\mathrm{d}t] \tag{4}$$

$$\mu = \frac{eD}{k_BT} \tag{5}$$

We also track the time-dependent inverse participation ratio (IPR) that measures the charge delocalization length along the polymer chain

$$\mathrm{IPR}(t) = \frac{1}{N_{\mathrm{traj}}}\sum_i^{N_{\mathrm{traj}}} \frac{1}{\sum_k \langle k|\phi_a^{(i)}(t)\rangle^4} \tag{6}$$

$|k\rangle$ is any suitable local basis of the system as discussed below.

We model the polymer chains as one-dimensional arrays of N monomers (with open boundary conditions), each associated with one electronic state $|k\rangle$. Although the model can easily be extended, we describe the ions via two effective, harmonic, classical vibrational degrees of freedom that modulate the site energy (local electron−phonon coupling) and electronic coupling (nonlocal electron−phonon coupling), respectively. The intramonomer mode x_k accounts for the changes in the monomer geometry upon addition of an excess charge, while intermonomer mode $\theta_{k,k'}$ describes the torsion between successive monomer units k and k' along the polymer axis. The onsite energy of monomer k gets linearly modulated with x_k by the coupling constant α_k while the electronic

https://dx.doi.org/10.1021/acs.jpclett.0c01793
J. Phys. Chem. Lett. 2020, 11, 6519−6525

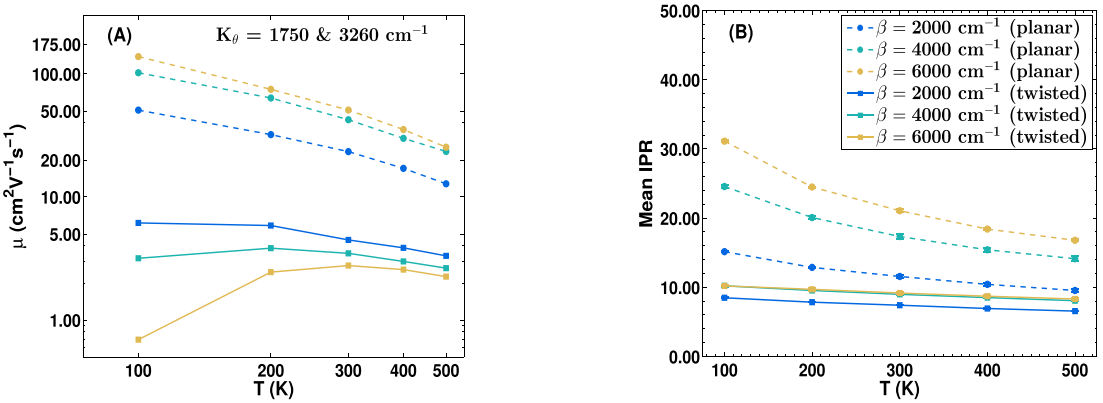

Figure 1. Temperature dependence of (A) charge-carrier mobility and (B) mean IPR within a single polymer chain at moderate (MD-derived torsional stiffness constants) K_θ = 1750 cm^{-1} and 3260 cm^{-1}. Broken lines with circles represent planar equilibrium configuration, while solid lines with squares represent twisted equilibrium configuration. Color codes for varying β are indicated in the figure. The lines are given only as a guide to the eyes.

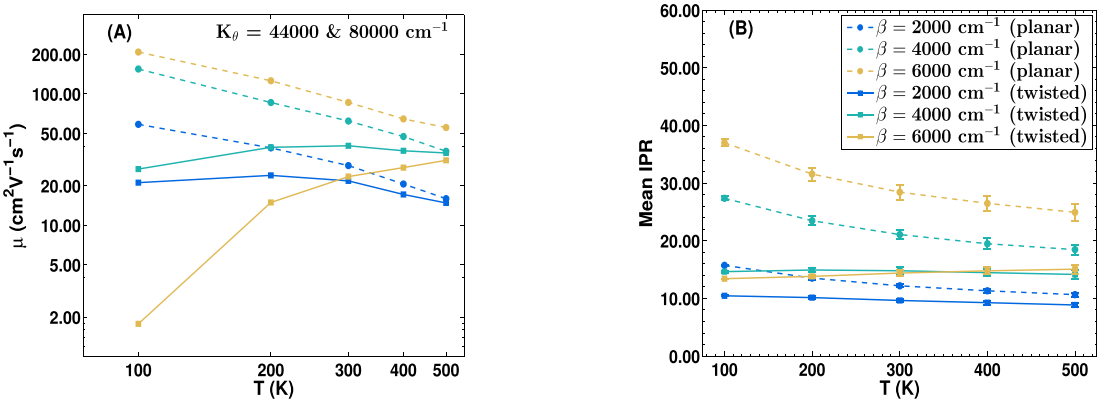

Figure 2. Temperature dependence of (A) charge-carrier mobility and (B) mean IPR within a single polymer chain at high K_θ = 44 000 cm^{-1} and 80 000 cm^{-1} (stiff torsional potentials). Color and symbol codes are similar to those in Figure 1.

coupling (i.e., the transfer integral) between nearest neighbors k and $k-1$ follows a sinusoidal evolution with $\theta_{k,k-1}$. The maximum electronic coupling (β) is achieved when $\theta_{k,k-1} = 0°$ or 180°. Thus, the total Hamiltonian ($H = H_e + H_n$) reads

$$H_e = \sum_{k=1}^{N} \alpha_k x_k |k\rangle\langle k| + \sum_{k=2}^{N} \beta|\cos(\theta_{k,k-1})| [|k\rangle\langle k-1| + |k-1\rangle\langle k|] \quad (7)$$

$$H_n = \sum_{k=1}^{N} \frac{1}{2}[mv_k^2 + I\omega_k^2 + K_x x_k^2] + \sum_{k=2}^{N} \frac{K_\theta}{2}(\theta_{k,k-1} - \theta_{eq})^2 \quad (8)$$

θ_{eq} being the equilibrium value of the intermonomer torsion angle in the neutral ground-state equilibrium configuration. K_x (K_θ) is the intramonomer vibrational force constant (intermonomer torsional stiffness constant) while v_k (ω_k) and m (I) correspond to the linear (angular) velocity and effective mass (moment of inertia) of monomer k.

Though our model is general enough that it can be applied to any conjugated polymer, we have first parametrized it against coarse-grained simulations performed on solid samples of P3HT. In a nutshell (see details in the Supporting Information), we have fitted the torsion potential in eq 8 to reproduce the results obtained by Boltzmann inversion of conformational populations derived from molecular dynamics (MD) simulations on large amorphous bundles of P3HT chains (16 polymer chains of 300 monomers). This leads to a double-well potential centered around $\theta_{eq} \approx 36°$ and $\theta'_{eq} \approx 153°$ with torsional stiffness constants K_θ = 1750 cm^{-1} and K'_θ = 3260 cm^{-1}, respectively. This asymmetry in the potential energy surfaces around anti versus syn conformations has been considered in the simulations, as detailed in the Supporting Information. Next, we have carried out density functional theory (DFT) calculations at the B3LYP/cc-pVDZ level on P3HT dimers with varying torsional angle between the monomer units employing the GAUSSIAN-16 package[43] (see details in the Supporting Information); the corresponding electronic structure has been successfully reproduced by our tight-binding approach considering $\beta \approx 3650$ cm^{-1} (that would translate into a full electronic bandwidth of $4\beta \approx 1.8$ eV at the infinite chain length limit, a very large but expected value for wide-band one-dimensional conjugated polymers).

The other parameters are taken either from previous charge transport studies on molecular crystals (K_x = 14500 amu ps^{-2}, α = 3500 cm^{-1}Å^{-1}, and γ = 100 ps^{-1})[6,39] or adjusted for thiophene rings (m = 80 amu and I = 29 amu Å^2). Thereafter, we refer to this set of parameters as the "P3HT model". Because we aim at deriving a general structure−property relationship pertaining to charge transport along conjugated polymer chains, we actually performed simulations for a broad range of parameters associated with the most relevant degrees of freedom and interactions, namely (i) the equilibrium torsion

https://dx.doi.org/10.1021/acs.jpclett.0c01793
J. Phys. Chem. Lett. 2020, 11, 6519−6525

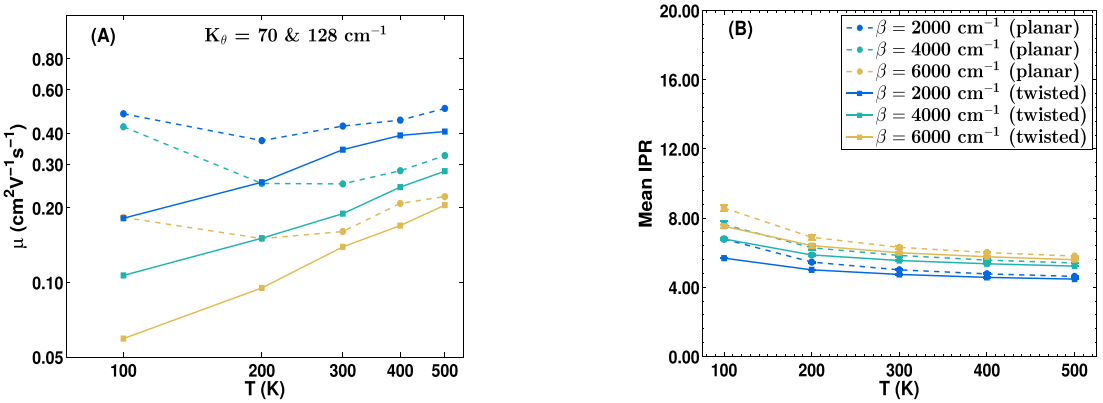

Figure 3. Temperature dependence of (A) charge-carrier mobility and (B) mean IPR within a single polymer chain at low K_θ = 70 cm^{-1} and 128 cm^{-1} (soft polymer backbone). Color and symbol codes are similar to those in Figure 1.

angle (taken to be either θ_{eq} = 36°/153° in P3HT chains or 0°/180° for planar chains) and the conformational stiffness (varied over 3 orders of magnitude in K_θ, corresponding to characteristic time scales with oscillation period 0.11 ps ≤ T ≤ 3.7 ps), along with (ii) the electronic coupling or bandwidth (with β varied from 2000 to 6000 cm^{-1}).

We start our analysis by exploring the temperature-dependent charge-carrier mobility and charge delocalization as this provides a useful hint into the transport mechanism, in addition to being a testbed for comparison to experiment. At first, we consider the case of polymer chains with planar equilibrium configurations, corresponding to equilibrium angles θ_{eq} = 0°/180° in eq 8. At moderate and high values of K_θ (stiff chain), $\mu(T)$ shows band-like transport (Figures 1A and 2A) with mobility decreasing with temperature following a power law, because of scattering with thermal phonons. Furthermore, the mobility values are found to be comparable to those reported for molecular crystals.[6] The charge carriers remain largely extended over the polymer chain (with a coherence length extending over ∼30 repeating units) (Figures 1B and 2B) and the mean IPR reduces with increasing T, thus remaining on par with $\mu(T)$. This is reminiscent of the picture prevailing in molecular crystals, as put forward by Troisi and co-workers,[44] where thermal fluctuations in the electronic coupling (here driven by changes in conformation) drive a transient localization of the charge carriers. We also find that μ displays the expected dependence on electronic bandwidth, i.e. larger electronic coupling stimulates more extended delocalization and, consequently, enhances mobility (Figures 1A and 2A). For low K_θ (soft chains), $\mu(T)$ shows a more complex behavior: it is thermally activated at $T \geq 200$ K, while it reduces with temperature at lower T following a power law (Figure 3A). We also note that the charge-carrier mobility is a few orders of magnitude smaller than that in the case of stiffer chains. In addition, the mobility values shrink when the electronic bandwidth increases, at odds with the expectations from the molecular crystal scenario. We associate the lower μ values and the anticorrelation between μ and β to the formation of shallow trap states stemming from the conformational disorder in the flexible polymer chains. At low T, the ions do not have enough kinetic energy to cross the energy barrier associated with local, stochastic variations in torsion angles, so that charge carriers get confined over conformational subunits of ∼5 monomer units in length (Figure 3B). In addition, the larger the β, the deeper the trap states, explaining the inverse dependence of μ on β.

Unexpected results are obtained when repeating these calculations, but now considering the twisted ground-state configuration (i.e., the MD-derived P3HT model). In soft polymer chains (low K_θ), $\mu(T)$ displays a T-activated hopping behavior over the entire temperature range (Figure 3A), irrespective of the bandwidth. The flexibility of the polymer backbone allows exploring a range of torsional conformations, with low-energy conformations acting as traps for the charge carriers. Thermal energy can be used to escape from the transient conformationally induced potential wells and an Arrhenius-like fit of the $\mu(T)$ values in Figure 3A yields an activation energy of ∼70−120 cm^{-1} that is comparable to the stiffness constant. Except at low T, we note that similar results are obtained for planar and twisted equilibrium geometries, which is reasonable in the case of shallow potentials. We also note that the T-dependence of the mobility in soft, twisted polymer chains is similar to the T-dependence of exciton diffusion coefficient in oligothiophene system observed by Binder et al., where the torsion-induced dynamical barriers get overcome by thermal energy.[32]

The most remarkable results are obtained at intermediate and large K_θ values (Figures 1A and 2A). There, the charge-carrier mobility shows an unexpected temperature dependence, with a strong thermally activated behavior at low T and a power-law dependence at high T (with a critical crossover T being a subtle function of K_θ and β). The temperature dependence is also significantly different from that predicted for planar chains (planar chains show a power-law dependence across the entire parameter space). Furthermore, there is no clear correlation between mobility and charge delocalization length, the latter being very weakly T-dependent (Figures 1 and 2). For these relatively stiff backbones, the classical forces felt by the ions tend to confine the system in regions close to the twisted equilibrium geometry, while the electronic forces favor more planar backbones. This interplay leads to a rather complex density of states, the width of which depends on the magnitude of electronic coupling β and where the low-energy states are on average more confined in space (see the Supporting Information). The mobility value is now primarily dictated by the probability for the thermalized carriers to reach higher-energy extended states (at the so-called mobility edge), which explains the initial increase of μ with T. At low T, the energy gap between the active state and the available adiabatic states indeed decreases with T (see the Supporting Information). This energy gap is also larger for higher β values, hence the unconventional decrease in mobility with

https://dx.doi.org/10.1021/acs.jpclett.0c01793
J. Phys. Chem. Lett. 2020, 11, 6519−6525

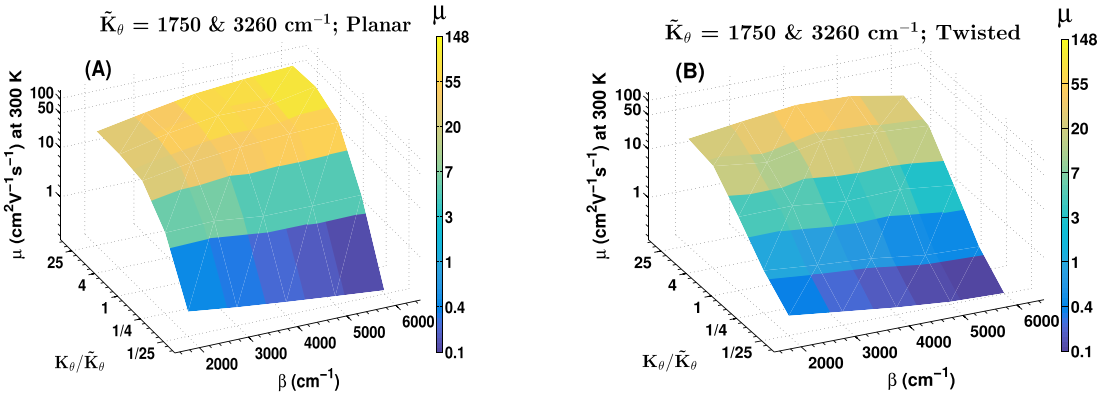

Figure 4. Room-temperature intrachain mobility for varying electronic bandwidth, β, and torsional stiffness, K_θ, in (A) planar equilibrium geometry and (B) twisted equilibrium geometry. Different K_θ are indicated in terms of ratio with the reference torsional stiffness of P3HT $\tilde{K}_\theta$ = 1750 cm^{-1} and 3260 cm^{-1}. Mobility values are color-coded and shown in the adjacent colorbar.

bandwidth. At higher T, extended states become readily available, irrespective of bandwidth, and a power law behavior is recovered as in the planar equilibrium geometry case. Furthermore, the calculated intrachain charge-carrier mobility values for very stiff twisted polymers resemble that earlier reported by Schmidt et al. in perfect P3HT crystals.[30]

To demonstrate the concerted effect of electronic bandwidth and polymer backbone stiffness on intrachain charge transport, we report in Figure 4A,B room-temperature (RT) charge-carrier mobility calculated for a broad range of β and K_θ values. It is quite evident that the RT mobility strongly depends on the torsional stiffness as well as the equilibrium configuration of the neutral chain. For planar configurations, the RT mobility gets enhanced with larger bandwidth (except at low K_θ) and torsional stiffness, whereas for twisted configurations, the mobility improves with increasing K_θ, yet the dependence on β is nontrivial. Therefore, in contrast to previous studies[45,46] and expectations, enhanced electronic coupling can be detrimental to charge transport along conjugated polymers, unless the torsional potential is very stiff and the equilibrium geometry is close to planarity. Recent experimental studies on stiff polymers like IDTBT[47] have revealed that the mobility follows a power-law dependence at high T and features a sharp decline at low T. We believe that this can be interpreted as a situation where the polymer backbone is stiff but has slightly twisted equilibrium ground-state conformation, which is supported by molecular dynamics investigations.[21] In addition, the experimentally measured mobility values (~2 cm^2/(V s)) are also in the range predicted by our theory for parameters relevant to the P3HT model.

In conclusion, employing a mixed quantum−classical model, we have explored the interplay between electronic coupling along the polymer backbone, the equilibrium conformation, and stiffness of the torsion potential on the (temperature-dependent) intrachain charge-carrier mobility. We have in particular demonstrated that the unusual evolution of the mobility with temperature (thermally activated behavior at low T and a power-law dependence at high T) is a fingerprint for polymer backbones that display stiff torsion potentials with nonplanar equilibrium geometries. By constraining the conformation to be fully planar while retaining a large stiffness constant, our calculations predict that the RT charge-carrier mobility in conjugated (co)polymers would crank up from the current ~1 cm^2/(V s) to values beyond 100 cm^2/(V s). Possible strategies to increase rigidity and enforce planarity would be to use larger fused-ring monomer units, to promote weak (e.g., H-bonding) interactions between successive monomer units and to link the repeating units by carbon−carbon double bonds, as proposed recently by McCulloch and co-workers.[48] In conjunction with first-principle simulations, we believe that our model can easily be extended to account for the atomistic details of the polymer chains (e.g., the presence of alternated donor and acceptor units in copolymers) and guide the synthetic efforts toward a new generation of amorphous yet high-mobility polymer materials.

■ ASSOCIATED CONTENT

Supporting Information

The Supporting Information is available free of charge at https://pubs.acs.org/doi/10.1021/acs.jpclett.0c01793.

(1) Computational details of the surface hopping technique; (2) coarse-grained molecular dynamics simulations of amorphous P3HT; (3) torsional potential calculation for solid P3HT chains; (4) calculation of the electronic coupling; (5) illustration of localized nature of the low-energy adiabatic states; (6) variation of energy gap between the active state and the available adiabatic states; (7) comparison of MSD expressions; (8) time evolution of MSD at various temperature (PDF)

■ AUTHOR INFORMATION

Corresponding Authors

Suryoday Prodhan − *Laboratory for Chemistry of Novel Materials, University of Mons, Mons 7000, Belgium;* orcid.org/0000-0002-9000-2928; Email: suryoday.prodhan@umons.ac.be

Linjun Wang − *Center for Chemistry of Novel & High-Performance Materials and Department of Chemistry, Zhejiang University, Hangzhou 310027, China;* orcid.org/0000-0002-6169-7687; Email: ljwang@zju.edu.cn

David Beljonne − *Laboratory for Chemistry of Novel Materials, University of Mons, Mons 7000, Belgium;* orcid.org/0000-0002-2989-3557; Email: david.beljonne@umons.ac.be

Authors

Jing Qiu − *Center for Chemistry of Novel & High-Performance Materials and Department of Chemistry, Zhejiang University, Hangzhou 310027, China*

Matteo Ricci − *MaterialX LTD., Bristol BS20XJ, United Kingdom*

https://dx.doi.org/10.1021/acs.jpclett.0c01793
J. Phys. Chem. Lett. 2020, 11, 6519−6525

Otello M. Roscioni − *MaterialX LTD., Bristol BS20XJ, United Kingdom;* orcid.org/0000-0001-7815-6636

Complete contact information is available at: https://pubs.acs.org/10.1021/acs.jpclett.0c01793

Notes

The authors declare no competing financial interest.

■ ACKNOWLEDGMENTS

S.P. acknowledges Yoann Olivier and Anton Pershin for useful discussions and suggestions. Computational resources have been provided by the Consortium des Équipements de Calcul Intensif (CÉCI), funded by the Fonds de la Recherche Scientifique de Belgique (F.R.S.-FNRS) under Grant No. 2.5020.11 and by the Walloon Region. The present research also benefited from computational resources made available on the Tier-1 supercomputer of the Fédération Wallonie-Bruxelles, infrastructure funded by the Walloon Region under the Grant Agreement No. 1117545. The work in Mons is financially supported by FNRS FLAG-ERA JTC 2017 project "MXene-organic semiconductor blends for high-mobility printed organic electronic devices - MX-OSMOPED". L.W. acknowledges support from the National Natural Science Foundation of China (Grant Nos. 21922305, 21873080, and 21703202). M.R. and O.M.R. acknowledge the European Unions Horizon 2020 Framework Programme for support under Grant Agreement No. 646176 (EXTMOS). Part of the work was performed on the computational resource ForHLR II funded by the Ministry of Science, Research and the Arts Baden-Wurttemberg and DFG ("Deutsche Forschungsgemeinschaft"). D.B. is a FNRS Research Director.

■ REFERENCES

(1) Ostroverkhova, O. Organic Optoelectronic Materials: Mechanisms and Applications. *Chem. Rev.* **2016**, *116*, 13279−13412.
(2) Sirringhaus, H. 25th Anniversary Article: Organic Field-Effect Transistors: The Path Beyond Amorphous Silicon. *Adv. Mater.* **2014**, *26*, 1319−1335.
(3) Brédas, J.-L.; Beljonne, D.; Coropceanu, V.; Cornil, J. Charge-Transfer and Energy-Transfer Processes in π-Conjugated Oligomers and Polymers: A Molecular Picture. *Chem. Rev.* **2004**, *104*, 4971−5004.
(4) Coropceanu, V.; Cornil, J.; da Silva Filho, D. A.; Olivier, Y.; Silbey, R.; Brédas, J.-L. Charge Transport in Organic Semiconductors. *Chem. Rev.* **2007**, *107*, 926−952.
(5) Worth, G. A.; Meyer, H.-D.; Köppel, H.; Cederbaum, L. S.; Burghardt, I. Using the MCTDH wavepacket propagation method to describe multimode non-adiabatic dynamics. *Int. Rev. Phys. Chem.* **2008**, *27*, 569−606.
(6) Wang, L.; Beljonne, D. Flexible Surface Hopping Approach to Model the Crossover from Hopping to Band-like Transport in Organic Crystals. *J. Phys. Chem. Lett.* **2013**, *4*, 1888−1894.
(7) Wang, L.; Prezhdo, O. V.; Beljonne, D. Mixed quantum-classical dynamics for charge transport in organics. *Phys. Chem. Chem. Phys.* **2015**, *17*, 12395−12406.
(8) Spencer, J.; Gajdos, F.; Blumberger, J. FOB-SH: Fragment orbital-based surface hopping for charge carrier transport in organic and biological molecules and materials. *J. Chem. Phys.* **2016**, *145*, 064102.
(9) Giannini, S.; Carof, A.; Ellis, M.; Yang, H.; Ziogos, O. G.; Ghosh, S.; Blumberger, J. Quantum localization and delocalization of charge carriers in organic semiconducting crystals. *Nat. Commun.* **2019**, *10*, 3843.
(10) Noriega, R.; Rivnay, J.; Vandewal, K.; Koch, F. P. V.; Stingelin, N.; Smith, P.; Toney, M. F.; Salleo, A. A general relationship between disorder, aggregation and charge transport in conjugated polymers. *Nat. Mater.* **2013**, *12*, 1038−1044.
(11) Noriega, R.; Salleo, A.; Spakowitz, A. J. Chain conformations dictate multiscale charge transport phenomena in disordered semiconducting polymers. *Proc. Natl. Acad. Sci. U. S. A.* **2013**, *110*, 16315−16320.
(12) Noriega, R. Efficient Charge Transport in Disordered Conjugated Polymer Microstructures. *Macromol. Rapid Commun.* **2018**, *39*, 1800096.
(13) McCulloch, I.; Heeney, M.; Bailey, C.; Genevicius, K.; MacDonald, I.; Shkunov, M.; Sparrowe, D.; Tierney, S.; Wagner, R.; Zhang, W.; et al. Liquid-crystalline semiconducting polymers with high charge-carrier mobility. *Nat. Mater.* **2006**, *5*, 328−333.
(14) Zhang, X.; Hudson, S. D.; DeLongchamp, D. M.; Gundlach, D. J.; Heeney, M.; McCulloch, I. In-Plane Liquid Crystalline Texture of High-Performance Thienothiophene Copolymer Thin Films. *Adv. Funct. Mater.* **2010**, *20*, 4098−4106.
(15) Anthony, J. E.; Brooks, J. S.; Eaton, D. L.; Parkin, S. R. Functionalized Pentacene: Improved Electronic Properties from Control of Solid-State Order. *J. Am. Chem. Soc.* **2001**, *123*, 9482−9483.
(16) Sakanoue, T.; Sirringhaus, H. Band-like temperature dependence of mobility in a solution-processed organic semiconductor. *Nat. Mater.* **2010**, *9*, 736−740.
(17) Kline, R.; McGehee, M.; Kadnikova, E.; Liu, J.; Fréchet, J. Controlling the Field-Effect Mobility of Regioregular Polythiophene by Changing the Molecular Weight. *Adv. Mater.* **2003**, *15*, 1519−1522.
(18) Pingel, P.; Zen, A.; Abellón, R. D.; Grozema, F. C.; Siebbeles, L. D.; Neher, D. Temperature-Resolved Local and Macroscopic Charge Carrier Transport in Thin P3HT Layers. *Adv. Funct. Mater.* **2010**, *20*, 2286−2295.
(19) Grozema, F. C.; Siebbeles, L. D. A. Charge Mobilities in Conjugated Polymers Measured by Pulse Radiolysis Time-Resolved Microwave Conductivity: From Single Chains to Solids. *J. Phys. Chem. Lett.* **2011**, *2*, 2951−2958.
(20) Cook, A. R.; Asaoka, S.; Li, X.; Miller, J. R. Electron Transport with Mobility, $\mu > 86$ cm 2 /(V s), in a 74 nm Long Polyfluorene. *J. Phys. Chem. Lett.* **2019**, *10*, 171−175.
(21) Venkateshvaran, D.; Nikolka, M.; Sadhanala, A.; Lemaur, V.; Zelazny, M.; Kepa, M.; Hurhangee, M.; Kronemeijer, A. J.; Pecunia, V.; Nasrallah, I.; et al. Approaching disorder-free transport in high-mobility conjugated polymers. *Nature* **2014**, *515*, 384−388.
(22) Wang, S.; Fabiano, S.; Himmelberger, S.; Puzinas, S.; Crispin, X.; Salleo, A.; Berggren, M. Experimental evidence that short-range intermolecular aggregation is sufficient for efficient charge transport in conjugated polymers. *Proc. Natl. Acad. Sci. U. S. A.* **2015**, *112*, 10599−10604.
(23) Tsao, H. N.; Cho, D. M.; Park, I.; Hansen, M. R.; Mavrinskiy, A.; Yoon, D. Y.; Graf, R.; Pisula, W.; Spiess, H. W.; Mullen, K. Ultrahigh Mobility in Polymer Field-Effect Transistors by Design. *J. Am. Chem. Soc.* **2011**, *133*, 2605−2612.
(24) Bronstein, H.; Chen, Z.; Ashraf, R. S.; Zhang, W.; Du, J.; Durrant, J. R.; Shakya Tuladhar, P.; Song, K.; Watkins, S. E.; Geerts, Y.; et al. Thieno[3,2- b]thiopheneDiketopyrrolopyrrole-Containing Polymers for High-Performance Organic Field-Effect Transistors and Organic Photovoltaic Devices. *J. Am. Chem. Soc.* **2011**, *133*, 3272−3275.
(25) Zhang, X.; Bronstein, H.; Kronemeijer, A. J.; Smith, J.; Kim, Y.; Kline, R. J.; Richter, L. J.; Anthopoulos, T. D.; Sirringhaus, H.; Song, K.; et al. Molecular origin of high field-effect mobility in an indacenodithiophenebenzothiadiazole copolymer. *Nat. Commun.* **2013**, *4*, 2238.
(26) Thomas, T. H.; Harkin, D. J.; Gillett, A. J.; Lemaur, V.; Nikolka, M.; Sadhanala, A.; Richter, J. M.; Armitage, J.; Chen, H.; McCulloch, I.; et al. Short contacts between chains enhancing luminescence quantum yields and carrier mobilities in conjugated copolymers. *Nat. Commun.* **2019**, *10*, 2614.

(27) Fornari, R. P.; Aragó, J.; Troisi, A. A very general rate expression for charge hopping in semiconducting polymers. *J. Chem. Phys.* **2015**, *142*, 184105.
(28) Fornari, R. P.; Blom, P. W.; Troisi, A. How Many Parameters Actually Affect the Mobility of Conjugated Polymers? *Phys. Rev. Lett.* **2017**, *118*, 086601.
(29) Grozema, F. C.; van Duijnen, P. T.; Berlin, Y. A.; Ratner, M. A.; Siebbeles, L. D. A. Intramolecular Charge Transport along Isolated Chains of Conjugated Polymers: Effect of Torsional Disorder and Polymerization Defects. *J. Phys. Chem. B* **2002**, *106*, 7791−7795.
(30) Lücke, A.; Ortmann, F.; Panhans, M.; Sanna, S.; Rauls, E.; Gerstmann, U.; Schmidt, W. G. Temperature-Dependent Hole Mobility and Its Limit in Crystal-Phase P3HT Calculated from First Principles. *J. Phys. Chem. B* **2016**, *120*, 5572−5580.
(31) Binder, R.; Lauvergnat, D.; Burghardt, I. Conformational Dynamics Guides Coherent Exciton Migration in Conjugated Polymer Materials: First-Principles Quantum Dynamical Study. *Phys. Rev. Lett.* **2018**, *120*, 227401.
(32) Binder, R.; Burghardt, I. First-principles quantum simulations of exciton diffusion on a minimal oligothiophene chain at finite temperature. *Faraday Discuss.* **2020**, *221*, 406−427.
(33) Binder, R.; Burghardt, I. First-principles description of intra-chain exciton migration in an oligo(para-phenylene vinylene) chain. II. ML-MCTDH simulations of exciton dynamics at a torsional defect. *J. Chem. Phys.* **2020**, *152*, 204120.
(34) Nematiaram, T.; Troisi, A. Modeling charge transport in high-mobility molecular semiconductors: Balancing electronic structure and quantum dynamics methods with the help of experiments. *J. Chem. Phys.* **2020**, *152*, 190902.
(35) Giannini, S.; Carof, A.; Blumberger, J. Crossover from Hopping to Band-Like Charge Transport in an Organic Semiconductor Model: Atomistic Nonadiabatic Molecular Dynamics Simulation. *J. Phys. Chem. Lett.* **2018**, *9*, 3116−3123.
(36) Wang, L. J.; Peng, Q.; Li, Q. K.; Shuai, Z. Roles of inter- and intramolecular vibrations and band-hopping crossover in the charge transport in naphthalene crystal. *J. Chem. Phys.* **2007**, *127*, 044506.
(37) Wang, L.; Akimov, A. V.; Chen, L.; Prezhdo, O. V. Quantized Hamiltonian dynamics captures the low-temperature regime of charge transport in molecular crystals. *J. Chem. Phys.* **2013**, *139*, 174109.
(38) Bai, X.; Qiu, J.; Wang, L. An efficient solution to the decoherence enhanced trivial crossing problem in surface hopping. *J. Chem. Phys.* **2018**, *148*, 104106.
(39) Qiu, J.; Bai, X.; Wang, L. Crossing Classified and Corrected Fewest Switches Surface Hopping. *J. Phys. Chem. Lett.* **2018**, *9*, 4319−4325.
(40) Qiu, J.; Bai, X.; Wang, L. Subspace Surface Hopping with Size-Independent Dynamics. *J. Phys. Chem. Lett.* **2019**, *10*, 637−644.
(41) Tully, J. C. Molecular dynamics with electronic transitions. *J. Chem. Phys.* **1990**, *93*, 1061−1071.
(42) Wang, L.; Qiu, J.; Bai, X.; Xu, J. Surface hopping methods for nonadiabatic dynamics in extended systems. *Wiley Interdiscip. Rev.: Comput. Mol. Sci.* **2020**, *10*, No. e1435.
(43) Frisch, M. J.; Trucks, G. W.; Schlegel, H. B.; Scuseria, G. E.; Robb, M. A.; Cheeseman, J. R.; Scalmani, G.; Barone, V.; Petersson, G. A.; Nakatsuji, H. et al. *Gaussian16*, revision C.01; Gaussian Inc.: Wallingford, CT, 2016.
(44) Troisi, A.; Orlandi, G. Charge-Transport Regime of Crystalline Organic Semiconductors: Diffusion Limited by Thermal Off-Diagonal Electronic Disorder. *Phys. Rev. Lett.* **2006**, *96*, 086601.
(45) Viani, L.; Olivier, Y.; Athanasopoulos, S.; da Silva Filho, D. A.; Hulliger, J.; Brédas, J. L.; Gierschner, J.; Cornil, J. Theoretical characterization of charge transport in one-dimensional collinear arrays of organic conjugated molecules. *ChemPhysChem* **2010**, *11*, 1062−1068.
(46) Olivier, Y.; Niedzialek, D.; Lemaur, V.; Pisula, W.; Müllen, K.; Koldemir, U.; Reynolds, J. R.; Lazzaroni, R.; Cornil, J.; Beljonne, D. 25th Anniversary Article: High-Mobility Hole and Electron Transport Conjugated Polymers: How Structure Defines Function. *Adv. Mater.* **2014**, *26*, 2119−2136.
(47) Schott, S.; Chopra, U.; Lemaur, V.; Melnyk, A.; Olivier, Y.; Di Pietro, R.; Romanov, I.; Carey, R. L.; Jiao, X.; Jellett, C.; et al. Polaron spin dynamics in high-mobility polymeric semiconductors. *Nat. Phys.* **2019**, *15*, 814−822.
(48) Onwubiko, A.; Yue, W.; Jellett, C.; Xiao, M.; Chen, H.-Y.; Ravva, M. K.; Hanifi, D. A.; Knall, A.-C.; Purushothaman, B.; Nikolka, M.; et al. Fused electron deficient semiconducting polymers for air stable electron transport. *Nat. Commun.* **2018**, *9*, 416.

https://dx.doi.org/10.1021/acs.jpclett.0c01793
J. Phys. Chem. Lett. 2020, 11, 6519−6525